

## The acoustic wavefield generated by a vessel sailing over ocean bottom cables

S. Hegna<sup>1</sup>, R. Milne<sup>2</sup>, B. Foseide<sup>2</sup>

<sup>1</sup> PGS; <sup>2</sup> AkerBP

### Summary

---

During the acquisition of an ocean bottom cable (OBC) survey on the Norwegian continental shelf, a line was acquired with the source vessel sailing directly over and along one of the ocean-bottom cables without triggering the airgun sources. These OBC data have been used to assess the feasibility of estimating the acoustic wavefield generated by a vessel from data recorded by receivers located on the seabed and using this wavefield for imaging the subsurface beneath the receivers. A 2D NMO stack along the vessel path has been made and compared against a line in the same location extracted from a 3D PSDM stack volume derived based on data acquired on a dense 12.5 x 12.5m shot grid using airguns. Most reflectors observed in the data acquired with airguns can be recognized in the data acquired without active sources even though the latter data represents only ten minutes of acquisition and very limited processing. This indicates that the method may be used for monitoring purposes. Especially in areas with permanent receiver installations, it may offer a low cost and low impact monitoring solution with an opportunity for much more frequent acquisition of time lapse data.

## The acoustic wavefield generated by a vessel sailing over ocean bottom cables

### Introduction

Estimating the acoustic wavefield generated by a vessel from towed streamer data, and using this wavefield for imaging the subsurface, was discussed in Hegna (2021) and Hegna (2022a). It may also be of interest to use the method with ocean-bottom cable / node (OBC/N) data. Especially in areas with permanent receiver installations, it may offer a low cost and low impact monitoring solution with an opportunity for much more frequent acquisition of time lapse data. A synthetic study discussed in Hegna (2022b), indicated that the method may work with OBC/N data, even with relatively sparse spatial sampling of receivers compared to typical towed streamer configurations. During the acquisition of an OBC survey on the Norwegian continental shelf, a line was acquired with the source vessel sailing directly over and along one of the ocean-bottom cables without triggering the airgun sources. The sail line was approximately 900 m long. The receiver spacing along each ocean-bottom cable was 50 m, with hydrophone and three-component geophone sensors at each receiver location. Seismic data were recorded continuously, and it took approximately ten minutes to acquire the line. The temporal sampling rate in the recorded data was one milli-second. Recorded hydrophone data from four adjacent ocean-bottom cables are shown in Figure 1. These OBC data have been used to assess the feasibility of estimating the acoustic wavefield generated by a vessel from data recorded by receivers located on the seabed and using this wavefield for imaging the subsurface beneath the receivers.

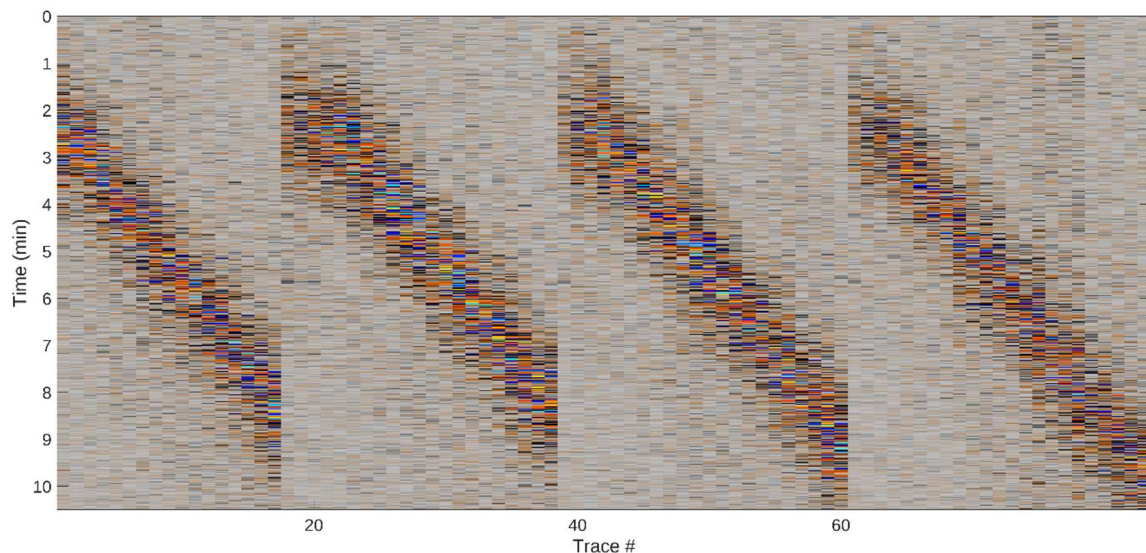


**Figure 1** Recorded hydrophone data from four adjacent ocean bottom cables with a 50-100 Hz band-pass filter to highlight the signals coming from the vessel.

### Method

The method for estimating the acoustic wavefield generated by a vessel, discussed in Hegna (2021, 2022a and 2022b), is based on first isolating the signals coming directly from the direction of the vessel, in other words the direct arrivals. Secondly, the isolated signals are backpropagated to the location(s) from where they were generated. The locations of the receivers as well as the source, i.e., the vessel, need to be known. The locations of the receivers were known. However, vessel positions were not recorded during the acquisition of this OBC dataset. Therefore, the locations had to be derived from the recorded seismic data. Initial source positions were estimated from the amplitudes in the recorded hydrophone data between 50 and 100 Hz. Figure 1 shows the amplitude build-up when the vessel was close to the receivers. The accuracy of these positions could be further improved from the recorded three-component geophone data through vector rotation such that one of the components was pointing in the direction directly towards the vessel as a function of time. The positions were optimized by maximizing the energy in the component pointing towards the vessel and minimizing the energy in the other two orthogonal components. Figure 2 shows three component geophone measurements after

vector rotation such that the original vertical component is pointing in the direction towards the vessel as a function of time.

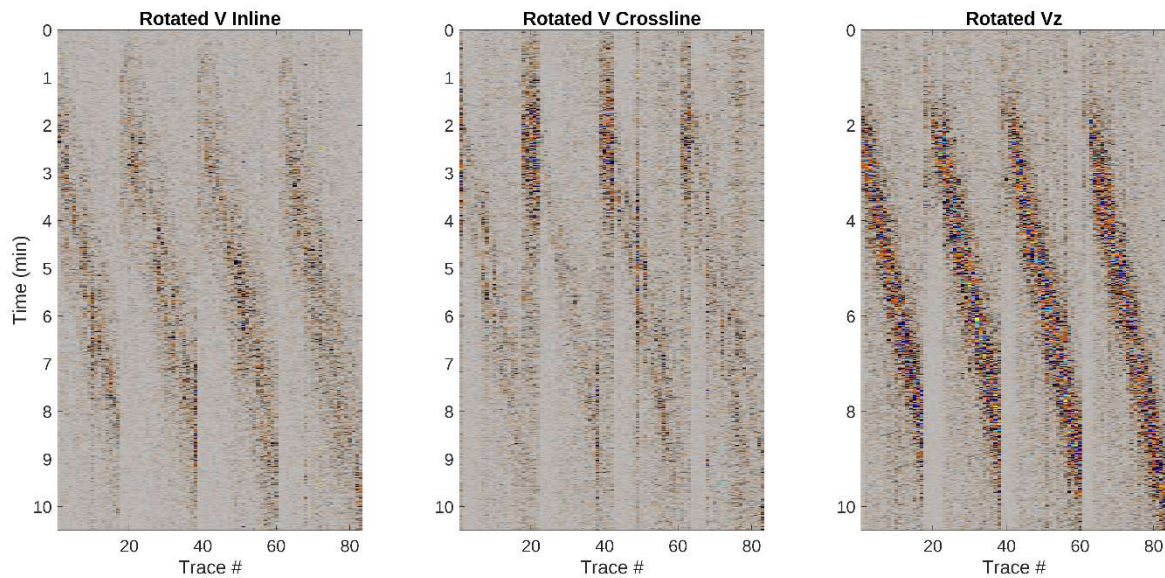


**Figure 2** Three component geophone measurements from four adjacent ocean bottom cables with a 50-100Hz band-pass filter after vector rotation such that the original vertical component is pointing in the direction towards the vessel as a function of time (right panel).

The component pointing in the direction towards the vessel sailing over the receivers should record the same direct arrivals associated with the wavefield generated by the vessel as recorded by the hydrophone, with a scalar applied to the motion sensor data related to the acoustic impedance and the difference in sensitivity between the hydrophones and the geophones. This scalar was determined by minimizing the energy of the difference between the hydrophone data and the rotated geophone component. Figure 3 shows the hydrophone data, the rotated geophone component after scaling by a factor 6.0668, and the difference between the hydrophone and the scaled and rotated geophone measurement.

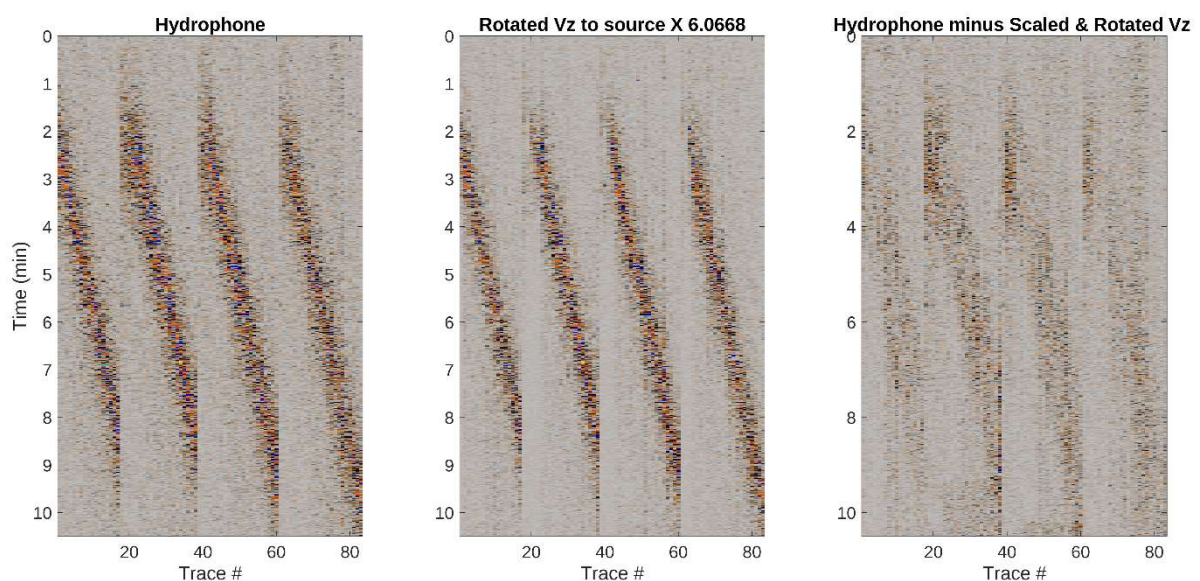


**Figure 3** Hydrophone data (left), scaled and rotated geophone data pointing in the direction towards the vessel (middle), and the difference between these (right).

The comparison in Figure 3 shows that there is little difference between the hydrophone data and the rotated geophone data after scaling the geophone data with this factor. The locations of the individual point sources needed to describe the directional characteristics of the acoustic wavefield generated by the vessel, and the signals emitted from each of these locations, were estimated using an iterative method presented in Hegna (2022a) and discussed in Hegna (2022b). Figure 4 shows the time series and the amplitude spectrum of the estimated signals emitted in the vertical direction.

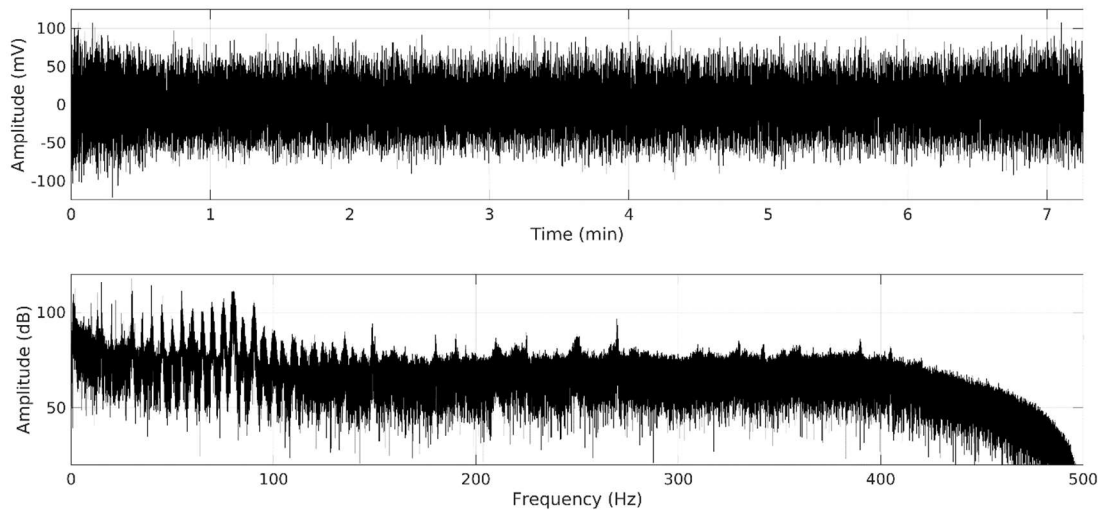


**Figure 4** Time series of the estimated wavefield generated by the vessel emitted in the vertical direction (top), and the amplitude spectrum of this time series (bottom).

The estimated acoustic wavefield was deconvolved from the upgoing pressure field in each receiver location after a receiver side wavefield separation performed using the scalar derived after vector rotation as discussed above. Three adjacent common receiver gathers are shown in Figure 5. The trace spacing of the common receiver gathers along the vessel path output from the source deconvolution was chosen to be 1.5625 m, to prevent spatial aliasing up to 475 Hz. This resulted in a common mid-point (CMP) spacing of 0.78125 m.

## Results

The resulting common receiver gathers were sorted into two-dimensional CMP gathers based on selected receivers along the vessel path. The average fold coverage was 11, and the offset ranges varied between +/- 400m to between 0 and 900m depending on where the vessel was relative to the locations of the receivers.

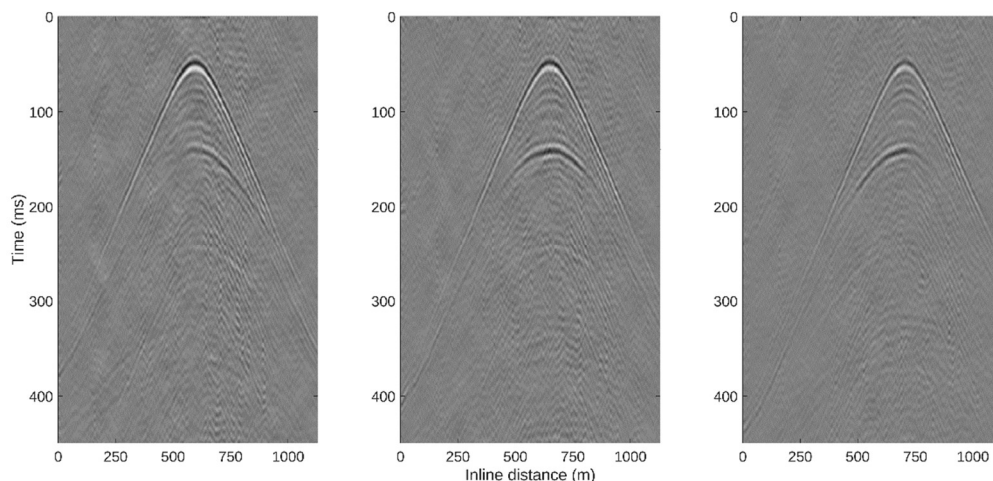


**Figure 5** Three adjacent common receiver gathers with 1.5625 m trace spacing within each gather.

The CMP gathers were NMO corrected and stacked using an existing velocity model and a 30° angle mute. Figure 6 shows a comparison between the line from a 3D PSDM volume acquired with airguns on a 12.5 x 12.5 m shot grid, with the NMO stack based on the data recorded without airguns. Most reflectors observed in the data acquired with airguns can be recognized in the data acquired without active sources even though the latter data represents only ten minutes of acquisition and very limited processing.

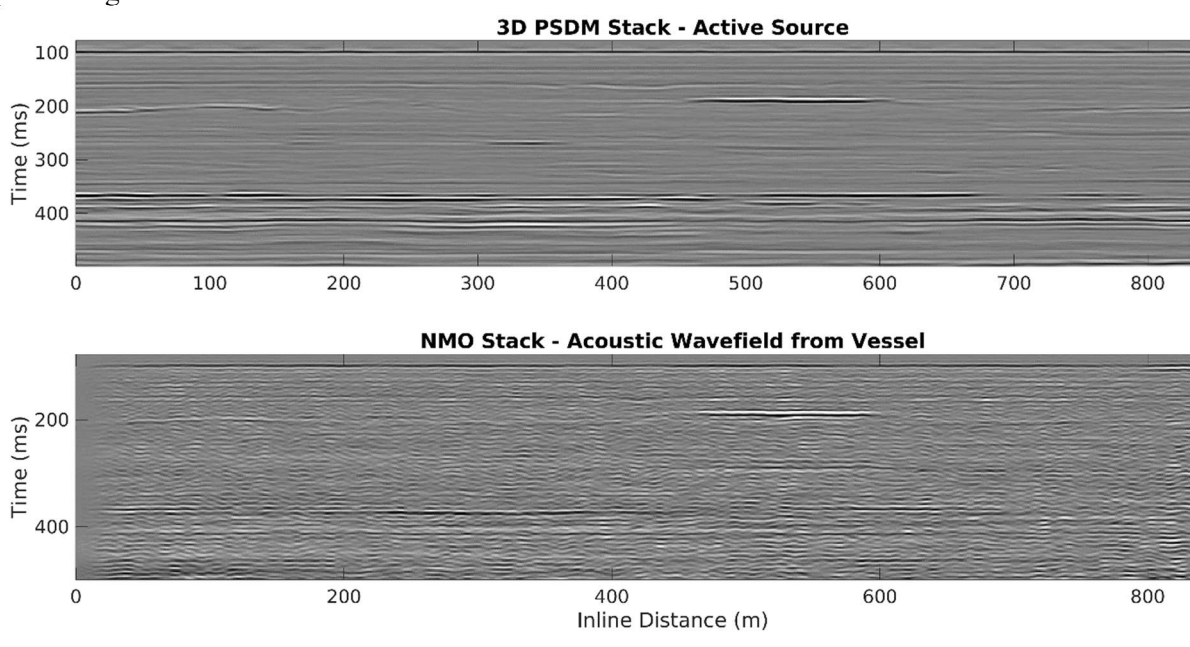


**Figure 6** The line along the vessel path from the 3D PSDM stack volume acquired with airguns (top), and the NMO stack of the data using the acoustic wavefield generated by the vessel as a source (bottom).

## Conclusions

Seismic data have been recorded while a vessel was sailing directly above an ocean bottom cable without using active sources. The source locations needed to get the directional characteristics of the wavefield generated by the vessel, as well as this acoustic wavefield, have been determined from the seismic data. The estimated acoustic wavefield generated by the vessel has been deconvolved from the received upgoing pressure field after a wavefield separation. A 2D NMO stack along the vessel path has been made and compared against a line in the same location extracted from a 3D PSDM stack volume derived based on data acquired on a dense 12.5 x 12.5m shot grid using airguns. The image obtained using the acoustic wavefield from the vessel exhibits similar features to the active source image, thereby indicating that the wavefield from the vessel could be used for monitoring purposes.

## Acknowledgements

Many thanks to AkerBP, license partner Pandion Energy, and PGS for permission to publish the results.

## References

- Hegna, S. [2021] Continuous wavefields method – The acoustic wavefield generated by the seismic vessel. 82<sup>nd</sup> Conference and Exhibition, EAGE, Extended Abstracts, 2021, 1-5.
- Hegna, S. [2022a] The acoustic wavefield generated by a vessel sailing on top of a streamer spread. 83<sup>rd</sup> Conference and Exhibition, EAGE, Extended Abstracts, 2022, 1-5.
- Hegna, S. [2022b] Imaging the subsurface using acoustic signals generated by a vessel. *First Break*, **40**(11), 47–53.